gel surface were barely touching. The state under laser irradiation was measured from the true lateral surface of the gel by direct thermography at the distance of 30 cm from the lateral surface of the gel. Thus, we accomplished 2-D temperature mapping of the gel. Tests were performed with a sample size of $n = 8$ in each group at three different stress amplitudes and thermal loads.

As the effect from photoacoustics, stress amplitude ($P(t)$) was calculated from Equations (1) and (2) below with piezoelectric film data [16]:

$$F(t) = \frac{V(t) \times (Cd + Cp)}{dt} \quad (1)$$

$$P(t) = 54.2 \times V(t) \quad (2)$$

$F(t)$, detected stress at transducer; $V(t)$, output voltage of transducer; Cd, loading capacitance of oscilloscope; Cp, capacitance of transducer; dt, strain constant for PVdF.

For photoacoustics, thermal load (Ω) was defined as in Equation (3) below and calculated by integrating the volume of the portion that reached a temperature $\geq 50°C$ on thermography [15]:

$$\Omega = \int (> =''°C \text{ volume ratio}) \delta\tau \quad (3)$$

DNA Content as a Marker of Residual Cells

DNA content was used as an index of residual cell count in wells. Cells were harvested after irradiations and treated with a papain solution at 60°C overnight. The papain solution was prepared by dissolving papain at a concentration of 125 μg/ml in 0.1 M phosphate-buffered saline (pH 6.0) with 5 mM cysteine–HCI and 5 mM Na_2 EDTA. The DNA content in specimens was then determined according to the methods of Kim et al. [17] by fluorometric assay using Hoechst 33258 (Polyscience, Warrington, PA).

Evaluation of Damage to the Plasma Membrane

Lactate dehydrogenase (LDH) is a stable cytoplasmic enzyme present in all cells, and is rapidly released into the cell culture supernatant upon damage to the plasma membrane. Levels of this enzyme thus reflect loss of membrane integrity and offer an indicator of cell death. Using a Cytotoxicity Detection Kit (Boehringer Mannheim), LDH release was measured in culture supernatants by enzyme-linked immunosorbent assay [18,19]. This test was performed with a sample size of $n = 8$ in each group. LDH rate was calculated according to formula (4):

$$\text{LDH realease (\%)} = \frac{[\text{experimental value} - \text{low control value}]}{[\text{high control value} - \text{low control value}]} \times 100 \quad (4)$$

Evaluation of Matrix Synthesis Ability

Proteoglycan synthesis was used as an index of matrix synthesis, and was measured by rapid filtration assay of ^{35}S incorporation [20]. The three-dimensionally cultured cells and DMEM containing ^{35}S-sulfate at l0 μCi/ml were incubated for every 12 hours (12-hour pulse labeling) from 0 to 48 hours after laser irradiation, and quantified by scintillation counting. This assay was applied to measure the matrix-synthesizing ability of damaged target cells. This test was performed with a sample size of $n = 8$ in each group.

RESULTS

Residual Cell Count

When the amount of vaporization from the laser is large, the residual cell count (%DNA content) is low. In the 54-J total energy group, this value was 60–70%, and tended to decrease as the amount of energy per shot increased. In the 27-J group, in contrast, %DNA content was about 80% in all cases. Residual cell count thus tended to be higher in the 27-J group with a small amount of vaporization (Fig. 2).

Cell Damage

In the 27-J group, LDH release was 10–35% and the injury to cells was mild. The value was particularly low 12 hours after irradiation, at about 10% in all cases, and little cytotoxicity was evident. In the 54-J group, high values of ≥40% were seen from 12 hours after irradiation, reaching ≥60% more than 24 hours after irradiation. Damage to cells was great (Fig. 3).

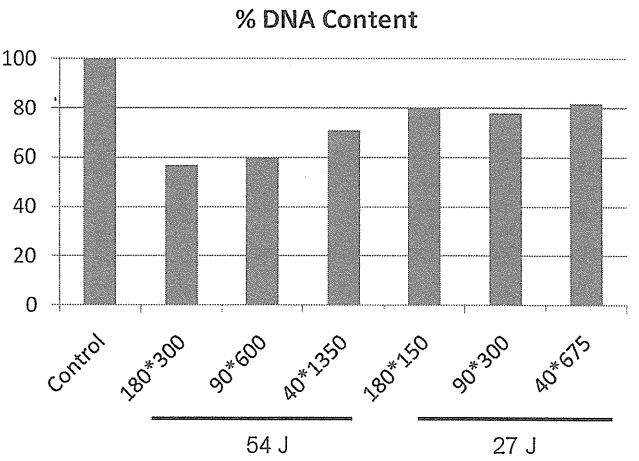

Fig. 2. Use of %DNA content as a marker of surviving cells after laser irradiation. In the 54-J total energy group ($n = 8$), %DNA content was 60–70%, and tended to decrease as the amount of energy per shot increased. In the 27-J group ($n = 8$), in contrast, %DNA content was about 80% in all cases. (e.g., 180 × 300: 180 mJ/pulse × 300 shots = total 54 J).

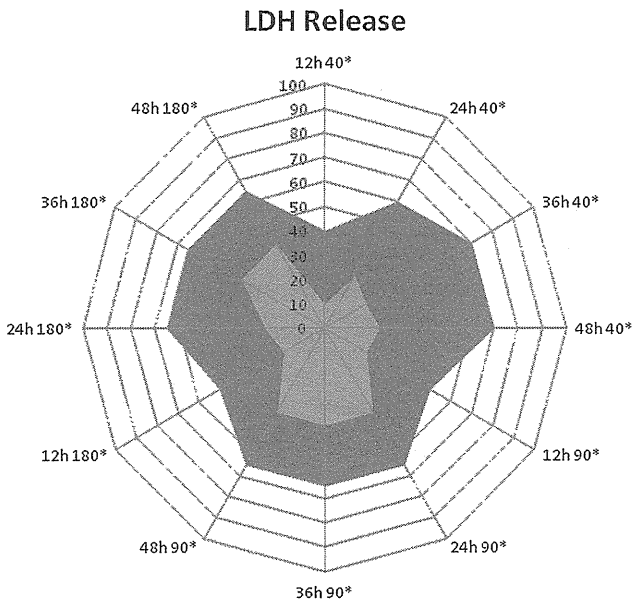

Fig. 3. LDH release as a marker of cell membrane damage. In the total energy 27-J group ($n = 8$), LDH release was 10–35% and the injury to cells was mild. In the 54-J group ($n = 8$), values were $\geq$40% from 12 hours after irradiation and reached $\geq$60% more than 24 hours after irradiation. The damage to cells was great. Red area: Groups of 54 J, Blue area: Groups of 27 J, (ex; 12 hours 40*; 40 mJ/pulse $\times$675 or 1,350 shots = total 27 J or 57 J irradiation after 12 hours).

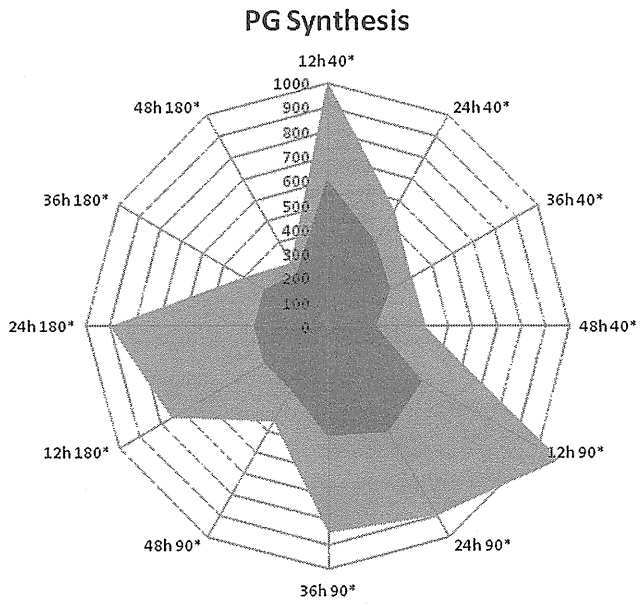

Fig. 4. Proteoglycan synthesis as a marker of synthesis of extracellular matrix. Proteoglycan synthesis was low overall in the 54-J group ($n = 8$), and synthesis was inhibited by the high level of cell damage. In the 27-J group ($n = 8$), in contrast, some cases showed high synthetic activity depending on the irradiation conditions. Red area: Groups of 54 J, Blue area: Groups of 27 J, (ex; 12 hours 40*; 40 mJ/pulse $\times$675 or 1,350 shots = total 27 J or 57 J irradiation after 12 hours).

Matrix Synthetic Capacity

Proteoglycan synthesis was low overall in the 54-J group, and synthesis was inhibited by the high level of cell damage. In the 27-J group, in contrast, cases of high synthetic activity were seen, depending on the irradiation conditions (Fig. 4). Matrix-synthesizing capacity at 12 hours after irradiation was large, and cell activity was thought to be modified considerably. In the 90-mJ/pulse condition in particular, activation of proteoglycan synthesis was maintained a long time after irradiation compared with other conditions.

Influence of Photoacoustic Effect

Figure 5 shows the relationship between the photoacoustic effect and LDH release and proteoglycan synthesis. Linear correlations were obtained in both the 27- and 54-J groups, and this experiment clarified the influence of the photoacoustic effect on cells. Proteoglycan synthesis in particular was thought to be susceptible to influences from the photoacoustic effect.

Influence of Photothermal Effect

Figure 6 shows the relationship between the photothermal effect and LDH release and proteoglycan synthesis. A weak linear correlation with LDH release was seen in the 54-J group, but no other correlations were seen in either the 27- or 54-J groups.

DISCUSSION

We have previously focused on the fact that the cells contained in intervertebral discs form a chondron-like morphology in tissue similar to articular cartilage, and confirmed that the biological status of these cells in the body could be reproduced in three-dimensional culture [21–23]. Then, by three-dimensional culture of the component cells of intervertebral discs, as an aggregate of heterogenous cells from the inner and outer layers of the intervertebral disc, a homogenous cytoplasm was obtained. The essentially different features of the inner and outer layers of the annulus fibrosus were confirmed to have been eliminated [21]. In other words, the uniform cell populations created by three-dimensional culture could be used to evaluate cell damage and matrix synthesis of cells in an environment similar to that of tissue. With the use of this three-dimensional model, complex cell reactions in the body resulting from laser irradiation can be evaluated *in vitro*.

From the results for DNA content and LDH release, damage to cells appeared mild in the 27-J group. However, findings suggested that in the 54-J group, necrosis occurs over a wide range out from the center in the early phase after irradiation. With proteoglycan synthesis, some cases showed maintenance of high synthetic activity over a long period depending on the irradiation conditions in the 27-J group. This indicates that with appropriate

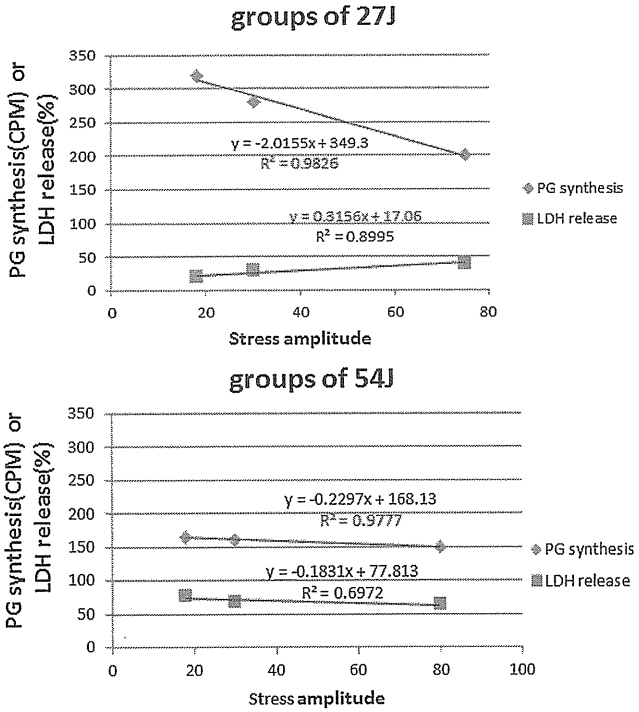

Fig. 5. Correlation between PG synthesis/LDH release and stress amplitude. Linear correlations were obtained in both the 27- and 54-J groups (n = 8 each). Proteoglycan synthesis in particular was considered susceptible to influences from the photoacoustic effect. Tests were performed at three different stress amplitudes.

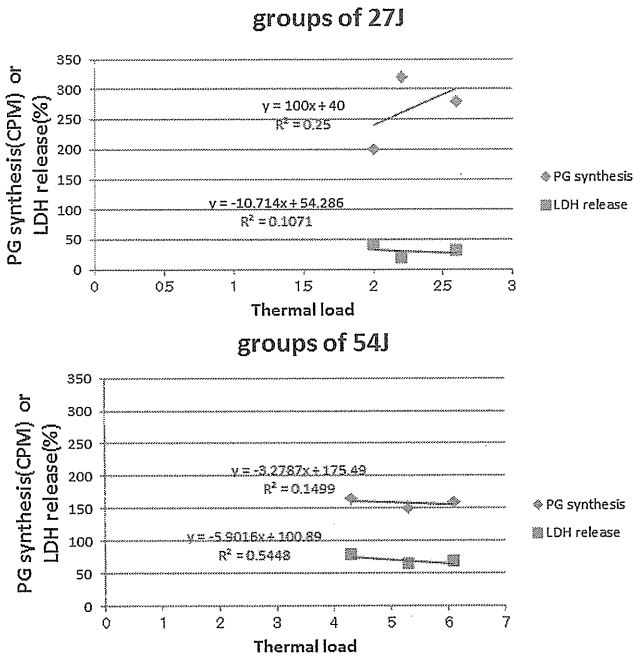

Fig. 6. Correlation between PG synthesis/LDH release and thermal load. A weak linear correlation with LDH release was seen in the 54-J group (n = 8), but no other correlations were found. Tests were performed in each group at three different thermal loads.

irradiation conditions, intervertebral disc cells are activated without causing total cell death, and local matrix synthesis flourishes, suggesting that this is a condition in which decreased pressure is obtained from tissue vaporization of the irradiation site with laser irradiation, while at the same time increasing the reparative abilities of the tissue around the irradiation site. Tissue damage from PLDD may thus be able to be minimized. This kind of cell activation effect does not exist in conventional percutaneous nucleotomy, in which the nucleus pulposus is extracted using a punch, and is thought to be a characteristic effect of laser irradiation. In an actual clinical situation, we believe that laser irradiation should not performed continuously from beginning to end. It should be performed in intervals; tissue-cooling time should be set; and laser irradiation should be broken up several times. Local heat retention needs to be monitored in a timely manner, but no medical devices currently enable detailed and appropriate monitoring of the laser irradiation tip. We look forward to the development of medical devices that enable monitoring of local status to provide clinical feedback on irradiation conditions, so that one of the characteristic effects of lasers, the elevation of proteoglycan synthesis, can be fully displayed.

A threshold level is known to exist in the thermal load. With 54 J, LDH release reaches ≥60% and proteoglycan synthesis is also low, suggesting that extensive damage occurs in many cells within environments that are already above the threshold. However, to understand the thermal load in greater detail, more refined methods will be necessary with closer monitoring, not just in the high range above a certain standard temperature (≥50°C in this study).

Laser irradiation produces both photothermal and photoacoustic effects, but the impact on cells is conjectured to differ depending on the total energy. Total energy is closely related to optimization of irradiation conditions, and irradiation conditions in the 27-J group are beneficial from the perspectives of a cytoprotective effect and promotion of matrix synthesis, and may be conditions that can be extrapolated to clinical practice. Evaluation methods in this study that enabled *in vitro* measurement and evaluation of cell reactions caused by both photothermal and photoacoustic effects from laser irradiation may be useful in optimizing laser irradiation conditions.

In conclusion, the three-dimensional culture model of intervertebral disc cells is excellent for clarifying the relationship between cell reactions, photoacoustic effect, and photothermal effect resulting from laser irradiation. In addition, total energy is closely related to optimization of irradiation conditions, and irradiation conditions in the 27-J group were beneficial from the perspectives of cytoprotection and promotion of matrix synthesis, and may be conditions that can be extrapolated to clinical practice.

ACKNOWLEDGMENTS

The authors thank Prof. Tsunenori Arai, Department of Applied Physics and Physico-Informatics, Faculty of Science and Technology, Keio University, Japan for providing useful information, comments, and technical critique with Ho:YAG laser irradiation.

REFERENCES

1. Choy DS, Case RB, Fielding W, Hughes J, Liebler W, Ascher P. Percutaneous laser nucleolysis of lumbar disks [letter]. N Engl J Med 1987;317:771–772.
2. Choy DS, Ascher PW, Ranu HS, Saddeknis S, Alkaitis D, Liebler W, Hughes J, Diwan S, Altman P. Percutaneous laser disc decompression. A new therapeutic modality [published erratum appears in Spine 1993; Jun 1;18(7):939]. Spine 1992;17:949–956.
3. Yonezawa T, Onomura T, Kosaka R, Miyaji Y, Tanaka S, Watanabe H, Abe Y, Imachi K, Atumi K, Chinzei T, Mabuchi K, Fujimasa I. The system and procedures of percutaneous intradiscal laser nucleotomy. Spine 1990;15:1175–1185.
4. Davis JK. Percutaneous discectomy improved with KTP laser. Clin Laser Mon 1990;8:105–106.
5. Gottlob C, KopcHok GE, Peng SK, Tabbara M, Cavaye D, White RA. Holmium:YAG laser ablation of human intervertebral disc: Preliminary evaluation. Lasers Surg Med 1992; 12:86–91.
6. Quigley MR, Shih T, Elrifai A, Maroon JC, Lesiecki ML. Percutaneous laser discectomy with the Ho:YAG laser. Lasers Surg Med 1992;12:621–624.
7. Sato M,Ishihara M,Arai T, et al. Use of a new ICG-dye-enhanced diode laser for percutaneous laser disc decompression. Lasers Surg Med 2001;29:282–287.
8. Niemz MH. Laser-Tissue Interactions Fundamentals and Applications (Third, Revised Edition). Biological and Medical Physics, Biomedical Engineering. Springer. 2004; XVI: 65.
9. Arai T. A review for new laser devices for laser therapy in gastroenterology. J Jpn Soc Laser Surg Med 1993;14:13–20.
10. Yoshikawa M, Nakajima A, Arai T, Kikuchi M, Kannari H, Obara M. The measurement of cavity collapse time by probe technique on water, agar, and vascular tissue during Ho:YAG laser contact ablation. Proc SPIE 1993;1882:382–387.
11. Tonami H, Kuginuki M, Kuginuki Y, et al. MR imaging of subchondral osteonecrosis of the vertebral body after percutaneous laser diskectomy. Am J Roentgenol 1999;173:1383–1386.
12. Uto Y, Mochida J, Nomura T. The clinical case study of postoperative condition on Percutaneous Laser Disc Decompression. Kanto J Orthop Traumatol 2003;34: 27–31.
13. Takeno K, Kobayashi S, Yonezawa T, Hayakawa K, Hachiya Y, Uchida K, Negoro K, Timbihurira G, Baba H. Salvage operation for persistent low back pain and sciatica induced by percutaneous laser disc decompression performed at outside institution: Correlation of magnetic resonance imaging and intraoperative and pathological findings. Photomed Laser Surg 2006;24:414–423.
14. Sato M, Ishihara M, Arai T, Asazuma T, Kikuchi T, Kikuchi M, Fujikawa K. Study for the optimum Ho:YAG laser irradiation condition on the percutaneous laser disc decompression (PLDD): In vitro quantitative evaluation of the influence on disc cells using three-dimensional cell culture system. Proc SPIE 1999;3601:387–391.
15. Sato M, Ishihara M, Arai T, Asazuma T, Kikuchi T, Kikuchi M, Fujikawa K. Study for the Ho:YAG laser—Intervertebral disc cell interaction using three-dimensional cell culture system. Proc SPIE 2000;3914:216–221.
16. Srinivasan R, Dyer PE, Braren B. Far-ultraviolet laser ablation of the cornea: Photoacoustic studies. Lasers Surg Med 1987;6(6) 514–519.
17. Kim YJ, Sah RL, Doong JY, Grodzinsky AJ. Fluorometric assay of DNA in cartilage explants using Hoechst 33258. Anal Biochem 1988;174:168–176.
18. de Luca A, Weller M, Fontana A. TGF-beta-induced apoptosis of cerebellar granule neurons is prevented by depolarization. J Neurosci 1996;16:4174–4185.
19. Dimmeler S, Haendeler J, Nehls M, Zeiher AM. Suppression of apoptosis by nitric oxide via inhibition of interleukin-1beta-converting enzyme (ICE)-like and cysteine protease protein (CPP)-32-like proteases. J Exp Med 1997;185:601–607.
20. Masuda K, Shirota H, THonar EJ. Quantification of 35S-labeled proteoglycans complexed to alcian blue by rapid filtration in multiwell plates. Anal Biochem 1994;217:167–175.
21. Sato M, Kikuchi T, Asazumz T, Yamada H, Maeda H, Fujikawa K. Glycosaminoglycan accumulation inprimary culture of rabbit intervertebral disc cells. Spine 2001;26:2653–2660.
22. Sato M, Asazuma T, Ishihara M, Kikuchi T, Masauoka K, Ichimura S, Kikuchi M, Kurita A, Fujikawa K. An atelocollagen Honeycomb-shaped scaffold with a membrane seal (ACHMS-scaffold) for the culture of annulus fibrosus cells from an intervertebral disc. J Biomed Mater Res 2003;64A: 248–256.
23. Sato M, Yamamoto Y, Sakai D, Mochida J. Characterization of intervertebral disc–disc cells and pericellular microenvironment. Clin calcium 2004;14:64–69.

整・災外 54：839—843，2011

新しい医療技術

ナノ秒パルスレーザーによる鏡視下関節軟骨の機能評価

佐藤正人[*1)] 石原美弥[*2)] 三谷玄弥[*1)]
沓名寿治[*1)] 菊地眞[*2)] 持田譲治[*1)]

要旨：関節軟骨本来の機能に基づく客観的評価方法が臨床の現場で欠如している。軟骨変性の進行は緩徐であり，評価方法のエンドポイントの設定も難しい。関節疾患の保存療法または術後評価は，患者の自覚症状やX線像での関節裂隙の狭小化の程度から推察しているに過ぎず，関節軟骨本来の機能に基づく客観的指標がないことで臨床評価が曖昧になることは，大きな問題である。関節軟骨本来の機能である力学特性（粘性，弾性，潤滑）と組織性状を正確に計測し，定量的に評価することが，より詳細な病態把握と治療効果判定に重要である。われわれは，定量的な関節軟骨機能の臨床診断法の確立を目指して，光音響原理に基づく力学特性評価と，時間分解自家蛍光スペクトル分析による組織性状評価の有効性を確認した。今後データを集積できれば，多角的に変形性関節症の詳細な病態把握が可能となり，患者に対して，よりきめ細かな治療計画の立案と遂行が可能となり，高齢者の健康寿命延伸に寄与するものと考える。

はじめに

関節疾患は，生命を直接脅かすものではないが，要支援となる原因疾患の第1位であり，ADLを下げるばかりかQOLの低下も招き，人的・社会的損失は計り知れない。低侵襲に関節軟骨本来の機能である力学特性と組織性状を正確に計測し，定量的に評価することができれば，変形性膝関節症をはじめとする軟骨変性を伴う運動器疾患の正確な病態把握と治療計画，ならびにその遂行が可能となるばかりか，新薬等の治験の際の客観的評価法としても有用と考えている。そして，臨床データの蓄積により，詳細な病態把握と予後診断が可能となり，個々の患者の病態に応じた，きめ細かな治療計画も可能となる。

本評価法は，平成17年度からの5カ年のNEDO事業「健康安心イノベーションプログラム/再生医療の早期実用化を目指した再生評価技術開発」で培った再生軟骨（組織工学的軟骨）の*in vitro*の非侵襲評価技術を発展させたものである。平成19年度から3カ年の厚労省科学研究費補助金（長寿科学総合事業）で継承し，世界で初めて実証した光音響原理に基づく力学特性評価と，時間分解自家蛍光スペクトル分析による組織性状評価による，関節軟骨機能の臨床診断技術の開発を目指したものである。

本研究で用いる計測技術は，“日本発・世界初”

*1) Masato SATO et al，東海大学医学部，外科学系整形外科学
*2) Miya ISHIHARA et al，防衛医科大学校，医用工学

Evaluation of articular cartilage using nanosecond pulsed laser under arthroscopy

Key words：Articular cartilage evaluation, Nanosecond pulsed laser, Arthroscopy

のもので，光音響原理に基づく粘弾性計測法の原理を提案し，検証実験でその有用性を確認したものである[1]。光音響信号を効率的に励起できる波長330 nmのパルスレーザーを使用することで，薬剤等の修飾なく測定可能な自家蛍光波長と時間を関数とした分析も可能となり，力学特性[2)~15)]と組織性状[16)~27)]とを同時に定量的に計測することが可能な技術を開発した[17]。本計測技術は当初，組織工学的に作製した再生軟骨の移植前の *in vitro* 評価法として確立した[3)~6)]。しかし，実際の臨床で，関節軟骨の診断において使用しなければならないのは，関節鏡視下環境であることが多い。

本研究においては，この評価技術を関節鏡視下で実施可能なレベルまでスケールダウンすることから始まった。つまり，励起用レーザー光の導光系と光音響信号と自家蛍光の検出センサーを一体化し，関節内計測用の曲げプローブを開発し，さらに，測定プロトコールの最適化によりハイスループットな計測を目指した。これらの実現により，臨床へのアプリケーションは大いに拡大された。すなわち，再生医療の評価技術として用いるばかりでなく，高齢者の多くに認められる軟骨変性の診断のために，関節軟骨本来の力学特性と組織性状とに基づく，関節鏡視下で定量評価可能な新規の軟骨機能診断法として，疾患病態の解明と治療効果判定に威力を発揮するものと考えた。

Ⅰ．原理と方法

光やレーザー光を計測対象である生体へ照射する結果として，散乱，反射，ならびに吸収に伴う温度上昇，さらには蛍光や音響波発生等が主な作用として挙げられる。最近注目されている光を利用した経ファイバー的，非侵襲的，選択的な診断補助装置は，このようなレーザー光と生体との相互作用の特長を生かした技術に立脚している[17]。本評価法で使用している軟骨の粘弾性計測のための光音響法は応力波発生という現象を利用したphotoacoustic な作用を利用したものであり，一方，軟骨の性状評価のための自家蛍光スペクトル解析は蛍光発生という現象を利用したphoto-chemical な作用を利用したものである[23)26)27)]。同一のレーザーが生体との間で異なる相互作用を生じるため，これらの相互作用を利用することで，形態情報だけでなく，生理的，生化学的な多くの情報をも同時取得することが可能であることから，超音波のような単一情報の解析よりも，診断装置としての将来性が大いに見込まれている。

われわれは，関節軟骨の本来の機能特性である力学特性と組織性状を，ナノ秒パルスレーザー照射することにより，非侵襲的に得られる光音響信号と蛍光情報から評価する技術を開発し，関節鏡視下に適用可能とし，変形性関節症など軟骨変性を伴う慢性関節炎等の正確な病態把握と各種治療による効果判定の定量評価を可能とするシステムを開発することを考えた[18]。そのために，光音響法と時間分解スペクトル分析法に必要不可欠な各要素技術を臨床使用可能なレベルに押し上げ，さらに，プロトタイプ装置，プローブ，解析ソフトの開発，改良を行い，実際の臨床の現場での術者の使用感もフィードバックするようにした。

Ⅱ．研究結果

1．光音響法による力学特性評価法

レーザー照射により，局所で発生した応力波が組織内を伝播する過程で組織固有の粘弾性により減衰する現象に着目し，光音響法で力学特性を計測できる基本原理を提案した。研究開発当初はレーザー光の至適な波長が不明であったため，コラーゲンやタンパクを光の吸収体として考慮し，実用性を考慮すると，小型，可搬，安価な励起光源が望まれるため，Qスイッチ Nd：YAG レーザーの第3高調波（波長：355 nm，パルス幅：5～6ns）を使用したシステムとした[2)~4)]。出力光は石英光ファイバー（コア径：400 nm）で導光し，光音響波の検出には，圧電性高分子フィルムのポリフッ化ポリビニリデン共重合体〔P（VdF/TrFE）〕を用いたプローブを開発した。これは，光ファイバーをプローブの中央に配置して，センサーをその周囲にリング状に配置して一体化した反射型プローブであり関節鏡視下でも計測可能なものである。

2．時間分解自家蛍光スペクトル解析による組織性状評価法

時間分解自家蛍光計測（TR-LIFS）においても，光音響法と同様に，励起光は光ファイバーで導光したQスイッチNd：YAGレーザー第3高調波を用い，ナノ秒オーダーのゲートで測定可能な分光システムを4チャンネルのデジタルパルスジェネレータで制御しながら施行した[16)~25)]。計測パラメータは，蛍光ピーク強度，半値幅，ピーク波長，蛍光体積，蛍光寿命を算出した。関節軟骨は，Ⅱ型コラーゲンに近似したスペクトルを呈し，ピーク波長ならびに半値幅も近似した。一方，椎間板線維輪外層はⅠ型コラーゲンに近似したスペクトルを呈し，同様にピーク波長ならびに半値幅も近似した[16)17)]。これらの結果は，生体内の自家蛍光物質であるコラーゲンの組成までも，非接触で計測可能であることを示したものであり，特に軟骨の変性度の診断に関してはⅠ型，Ⅱ型コラーゲンの含有比は重要と考えられており，これらを非侵襲的に計測可能な技術開発は軟骨評価法として意義深い。

3．臨床応用

本研究事業で開発した技術を用いて，東海大学医学部付属病院で関節鏡手術の際に臨床応用を施行している。細径化したプローブを用いて，関節鏡の術中のモニター表示画面の一部に計測波形をリアルタイムにモニター表示して術者が計測を実感できるように工夫した。この波形表示の仕方は，モニター中に大きくも小さくも可能である（図1）。

本計測法は，関節鏡視下の水中でも，関節を切開したオープンサージェリー，すなわち空気中でも実施可能である。粘弾性計測と同時に，関節軟骨の厚さも計測しているが，その際に音速で近似しているため，その部分で水中と空気中で，わずかな誤差が生じるが臨床で扱う計測結果としては問題とならない。

以下に臨床症例の計測結果表示例を提示する（図2）。関節鏡視下所見をOuterbridge classificationで，軟骨損傷程度をICRS分類で示したが，計測した光音響法での波形と軟骨の厚さ，および時間分解自家蛍光スペクトルを提示する。軟骨変性が進むとともに応力緩和時間τは延長し，粘性が大きくなる傾向にあった。また軟骨の厚さも変性とともに減少し，自家蛍光スペクトルはシャープなものからややブロードな二峰性を呈するようになった。

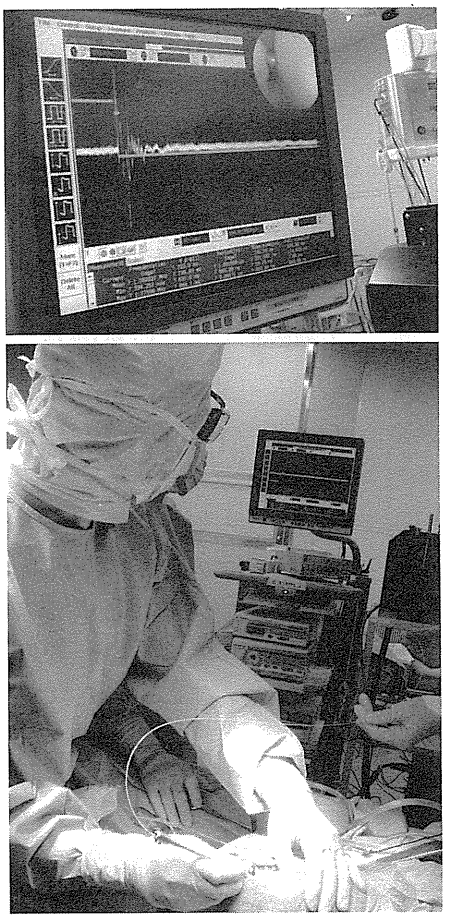

図1　手術時の計測状況

Ⅲ．考　察

本評価法は，関節鏡視下環境を必要とするが，粘弾性特性，性状評価，軟骨の厚さや表面構造の評価なども定量化でき，軟骨の評価に有用な情報を一気に得られる点が特に優れていると考えられる。光は選択するレーザーの波長や種類で非常に守備範囲の広いモダリティであり，そのため各種のモダリティとの併用あるいは融合が可能である。それによって，さらに正確な軟骨の診断が可能になると期待している。つまり，関節全体を描

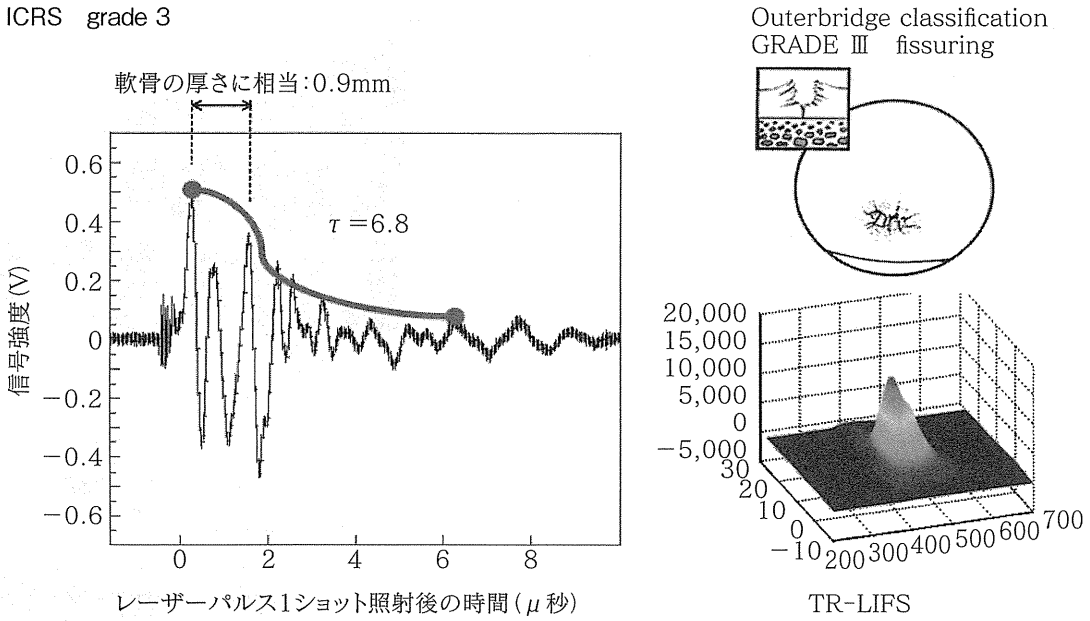

図 2 鏡視下軟骨計測の結果

出できるような画像構築に優れたモダリティと組み合わせれば,軟骨の変性度やその広がり具合も,画像とともに定量的に評価でき,変形性関節症のstructure modifying effectが評価可能となり,初めて適正な治療効果の判定が可能となるのではないかと考えている。

われわれは,本研究事業を通して,非侵襲的な微弱なパルスレーザーを用いて,関節鏡視下に関節軟骨の力学特性と性状評価を同時に施行可能であることを示した。そして,現在その標準化と実用化に向けて,試行錯誤を繰り返しながら取り組んでいる。本評価技術が実用化され,関節鏡視下で関節軟骨本来の機能である力学特性と組織性状を,整形外科医が正確に定量的に機能評価することが可能となれば,変形性関節症の正確な病態把握が可能となり,病態,病期ごとのきめ細かな治療法が確立し,根治の可能性が見えてくるのではないかとわれわれは考えている。さらに,各種の薬剤等の治療効果に関しても,従来の関節周囲の痛みやADL障害といった自覚症状に基づくものや炎症症状といった臨床症状の評価に加え,定量的に関節軟骨の力学特性と組織性状とを同時に計測し評価する本技術は,新薬等の治験の際の客観的評価法としても極めて有用と考えられる。つまり,従来エンドポイントが不明瞭な変形性関節症に対して,関節軟骨の変性の進行度(病期)を定量的に評価することで,構造修飾効果を客観的に評価し得るものと考える。また,各種モダリティ(特に画像診断装置)との組み合わせにより,本計測技術はさらに効果を発揮していくものと考える。

おわりに

関節鏡視下での観察や治療の際に,本計測により力学的評価と組織性状評価のデータが同時に多角的かつ定量的に今後集積されれば,軟骨変性診断の細分化が進み,そのgradeから各種の治療効果や予防対策などが明らかになるものと考える。

文　献

1) Ishihara M et al：Viscoelastic characterization of biological tissue by photoacoustic measurement. Jpn J Appl Phys **42**：556—558, 2003
2) Ishihara M et al：Development of a photoacoustic measurement method for the evaluation of regenerative medicine and tissue engineering for articular cartilage. J Jpn Soc Laser Surg Med **26**：53—59, 2005
3) Ishihara M et al：Usefulness of the photoacoustic measurement method for monitoring the

regenerative process of full-thickness defects in articular cartilage using tissue-engineering technology. Proc SPIE **5695**：288—291, 2005
4) Ishihara M et al：Usefulness of photoacoustic measurements for evaluation of biomechanical properties of tissue-engineered cartilage. Tissue Eng **11**：1234—1243, 2005
5) Ishihara M et al：Development of a noninvasive multifunctional measurement method using nanosecond pulsed laser for evaluation of regenerative medicine for articular cartilage. Proc SPIE **6084**：60840 V. 1—60840 V. 4, 2006
6) Ishihara M et al：Development of a diagnostic system for osteoarthritis using a photoacoustic measurement method. Lasers Surg Med **38**：249—255, 2006
7) 石原美弥ほか：再生医療評価・バリデーションのための非侵襲的計測法．生物工学会誌 **85**：438—441, 2007
8) 菊地　眞ほか：再生医療の基盤技術としての計測・画像工学．再生医療のためのバイオエンジニアリング，コロナ社，147—167, 2007
9) 石原美弥ほか:バイオメディカルイメージング．再生医療技術の最前線，シーエムシー出版，61—68, 2007
10) 石原美弥ほか:レーザーを用いた培養軟骨評価．再生医療に用いられる細胞・再生組織の評価と安全性，シーエムシー出版，123—137, 2007
11) Ishihara M et al：Multifunctional evaluation of tissue engineered cartilage using nano-pulsed light for validation of regenerative. IFMBE Proceedings WC **14**：3187—3189, 2007
12) 石原美弥ほか：ナノ秒パルスレーザーによる細胞外マトリックスの構築モニター．電気学会論文誌 **127-C**：2166—2170, 2007
13) Ishihara M et al：Usefulness and limitation of measurement methods for evaluation of tissue-engineered cartilage function and characterization using nanosecond pulsed laser. Proc SPIE **6439**：643909.1—643909.4, 2007
14) Ishihara M et al：Modification of measurement methods for evaluation of tissue engineered cartilage function and biochemical properties using nanosecond pulsed laser. Proc SPIE **6558**：685805.1—685805.5, 2008
15) Sato M et al：Recent technological advancements related to articular cartilage regeneration. Med Biol Eng Comput **46**：735—743, 2008
16) Ishihara M et al：Modification of measurement methods for evaluation of tissue-engineered cartilage function and biochemical properties using nanosecond pulsed laser. Proc SPIE **6858**：685804.1—685804.5, 2008
17) 佐藤正人ほか：変形性関節症の病態把握と治療効果判定を可能にする定量的機能診断システムの開発—ナノ秒パルスレーザーを用いた力学特性と組織性状の同時計測を目指して．別冊整形外科 No. 53：76—82, 2008
18) Ishihara M et al：Modification of measurement methods for evaluation of tissue engineered cartilage function and biochemical properties using nanosecond pulsed laser. Proc SPIE **6858**：685804.1—685804.6, 2008
19) 石原美弥ほか：再生医療を光で評価する．第4回集積光デバイス技術時限専門委員会誌 **IPD08**：44—49, 2008
20) Sato M et al：Recent technological advancements related to articular cartilage regeneration. Med Biol Eng Comput **46**：735—743, 2008
21) 石原美弥ほか：光による再生医療に用いる組織・細胞の評価．Microoptics News **26**：31—36, 2008
22) 石原美弥ほか：高齢者の ADL（Activity of Daily Life）維持に貢献する変形性関節症の早期診断システムの研究開発．未病と抗老 **18**：110—114, 2009
23) Kutsuna T et al：Noninvasive evaluation of tissue engineered cartilage with time-resolved laser-induced fluorescence spectroscopy. Tissue Eng Part C Methods **16**：365—373, 2009
24) Ishihara M et al：Multifunctional characterization of engineered cartilage using nano-pulsed laser. IFMBE Proc **25**：69—70, 2009
25) 石原美弥ほか：軟骨再生医療に有効な光技術．整・災外 **52**：1533—1537, 2009
26) Sato M et al：Development of a diagnostic system for osteoarthritis using a photoacoustic measurement method and tome-resolved autofluorescence. Bioengineering；Principles, Methodologies and Applications, Nova Science Publishers, 2010
27) Sato M et al：A diagnostic system for articular cartilage using non-destructive pulsed laser irradiation. Lasers Surg Med（in press）

Lasers in Surgery and Medicine 43:421–432 (2011)

A Diagnostic System for Articular Cartilage Using Non-Destructive Pulsed Laser Irradiation

Masato Sato, MD, PhD,[1]* Miya Ishihara, PhD,[2] Makoto Kikuchi, PhD,[2] and Joji Mochida, MD, PhD[1]
[1]*Department of Orthopaedic Surgery, Surgical Science, Tokai University School of Medicine, 143 Shimokasuya, Isehara, Kanagawa 259-1193, Japan*
[2]*Department of Medical Engineering, National Defense Medical College, 3-2 Namiki, Tokorozawa, Saitama 359-8513, Japan*

Background and Objectives: Osteoarthritis involves dysfunction caused by cartilage degeneration, but objective evaluation methodologies based on the original function of the articular cartilage remain unavailable. Evaluations for osteoarthritis are mostly based simply on patient symptoms or the degree of joint space narrowing on X-ray images. Accurate measurement and quantitative evaluation of the mechanical characteristics of the cartilage is important, and the tissue properties of the original articular cartilage must be clarified to understand the pathological condition in detail and to correctly judge the efficacy of treatment. We have developed new methods to measure some essential properties of cartilage: a photoacoustic measurement method; and time-resolved fluorescence spectroscopy.

Materials and Methods: A nanosecond-pulsed laser, which is completely non-destructive, is focused onto the target cartilage and induces a photoacoustic wave that will propagate with attenuation and is affected by the viscoelasticity of the surrounding cartilage. We also investigated whether pulsed laser irradiation and the measurement of excited autofluorescence allow real-time, non-invasive evaluation of tissue characteristics.

Results: The decay time, during which the amplitude of the photoacoustic wave is reduced by a factor of $1/e$, represents the key numerical value used to characterize and evaluate the viscoelasticity and rheological behavior of the cartilage. Our findings show that time-resolved laser-induced autofluorescence spectroscopy (TR-LIFS) is useful for evaluating tissue-engineered cartilage.

Conclusions: Photoacoustic measurement and TR-LIFS, predicated on the interactions between optics and living organs, is a suitable methodology for diagnosis during arthroscopy, allowing quantitative and multidirectional evaluation of the original function of the cartilage based on a variety of parameters. Lasers Surg. Med. 43:421–432, 2011. © 2011 Wiley-Liss, Inc.

Key words: osteoarthritis; photoacoustic measurement; time-resolved autofluorescence spectroscopy; tissue-engineered cartilage

INTRODUCTION

Osteoarthritis is thought to affect about 30 million people in Japan [1], but is not a direct threat to life. However, this condition both affects activities of daily living and diminishes quality of life among sufferers, so the associated human and social loss is difficult to estimate. The disease involves dysfunction caused by cartilage degeneration, but objective methodologies of evaluation based on the original function of the articular cartilage are currently unavailable. Evaluations that are currently used to establish conservative therapies or the prognosis of surgery as a treatment for osteoarthritis are merely based on patient symptoms or the degree of joint space narrowing on X-ray images. Accurate measurement and quantitative evaluation of the mechanical characteristics of cartilage (viscosity, elasticity, and lubrication) are important, and the tissue properties of the original articular cartilage need to be recognized if the pathological condition is to be understood in detail and treatment effects judged accurately. The development of such evaluation technologies is thus required to facilitate a functional diagnosis of osteoarthritis. If these evaluations can be achieved non-invasively, an accurate understanding of the pathologies should be possible, allowing the planning and performance of treatments for locomotor apparatus diseases that accompany the degeneration of cartilage, such as osteoarthritis. Such evaluations would also be useful as objective tools in situations such as the clinical

Conflict of interest statement: None.
Contract grant sponsor: Takeda Science Foundation; Contract grant sponsor: General Insurance Association of Japan; Contract grant sponsor: Mitsui Sumitomo Insurance Welfare Foundation; Contract grant sponsor: High-Tech Research Centre Project for Private Universities; Contract grant sponsor: Ministry of Education, Culture, Sports, Science, and Technology of Japan; Contract grant sponsor: New Energy and Industrial Technology Development Organization; Contract grant sponsor: Japan Foundation for Aging and Health.
*Corresponding to: Dr. Masato Sato, MD, PhD, Department of Orthopaedic Surgery, Surgical Science, Tokai University School of Medicine, 143 Shimokasuya, Isehara, Kanagawa 259-1193, Japan. E-mail: sato-m@is.icc.u-tokai.ac.jp
Accepted 28 March 2011
Published online 15 June 2011 in Wiley Online Library (wileyonlinelibrary.com).
DOI 10.1002/lsm.21065

trials of new drugs. A better understanding of the pathological condition in detail and determination of prognosis based on a body of clinical data should thus be possible. This will in turn facilitate the careful planning of treatments according to the specific pathological conditions of individual patients, improving activities of daily living, and enhancing the lives of many people.

Recent studies have suggested ultrasonography (US) as a sensitive method for determining cartilage thickness [2,3], structural properties [4], surface roughness [5], and enzymatically induced, specific degeneration of the superficial collagen network [6–8]. Mechanically, the collagen network is primarily responsible for the dynamic properties of cartilage by constraining transversal expansion, whereas proteoglycans contribute predominantly to interstitial fluid flow and the equilibrium response of cartilage [9,10]. Structural and mechanical properties vary within and between different articular surfaces [11,12]. Hattori et al. [13,14], reported a method to assess joint cartilage using US. By limiting examination to the mechanical properties of joint surfaces, cartilage can be assessed by indentation testing [15–17]. For the clinical diagnosis of mechanical properties, as with indentation testing, US requires arthroscopy. Quantitative intra-articular US imaging [18–20] and Optical coherence tomography [21,22] have been already been applied in vivo during knee surgery. MRI excels at geographical mapping, and while one advantage is the ability to gather a wide variety of extra-articular data, unlike US or indentation testing, viscoelastic properties cannot be directly measured. Normal and abnormal signals on images are simply compared to indirectly estimate mechanical properties. Several quantitative MRI techniques have recently been introduced for the non-invasive assessment of structural and mechanical properties of articular cartilage [23]. T2 mapping is sensitive to the integrity of collagen networks, collagen content, and fibril orientation [24–26]. T1 mapping in the presence of Gd-DTPA2 contrast agent, namely delayed gadolinium-enhanced MRI of cartilage (dGEMRIC), reflects the proteoglycan distribution in cartilage via the inverse distribution of ionic contrast agent [27,28].

The method of assessing cartilage function using a non-invasive pulsed laser that we have been analyzing is a technique focusing on interactions with the body when the laser is applied to cartilage. In other words, this photoacoustic method is a technique for measuring viscoelastic properties based on how sound waves travel and attenuate through the body and resembles US. Time-resolved laser-induced autofluorescence spectroscopy (TR-LIFS) measures autofluorescence generated through other interactions, and analyzes the properties of characteristically collagen-rich cartilage tissue matrix using the same laser irradiation. In other words, with our proposed method employing pulsed laser irradiation, interactions are measured by two different methods to obtain more biological information than US or indentation testing (Table 1). Relaxation times as measured by the photoacoustic method agreed well with the intrinsic viscoelastic parameters, with a correlation coefficient of 0.98, when

TABLE 1. Comparison of Major Cartilage Measurement Devices

	Indenter	Ultrasound	Laser (LIPA + TR-LIFS)	MRI
Direct measurement of viscoelasticity properties	Possible (up to superficial layer) large impacts of force application and superficial layer	Possible (average from surface to deep layers)	Possible (average from surface to deep layers)	Unable
Assessment of surface structures (fibrillation, etc.)	Possible	Possible	Possible	Unable
Compostional information (collagen content)	Unable	Possible (imaging)	Possible (distinguishable COL1 and COL2)	Possible (imaging)
Arthroscopic environment	Necessary	Necessary	Necessary	Unnecessary

LIPA, laser-induced photoacoustic measurement; TR-LIFS, time-resolved laser-induced autofluorescence spectroscopy; COL1, collagen type 1; COL2, collagen type 2. Viscoelasticity can be measured directly using an indenter, ultrasound system, or laser. However, these devices all require arthroscopy. Conversely, MRI excels at geographical mapping and is advantageous for gathering a wide variety of extra-articular information, but the mechanical properties of abnormal signals can only be estimated indirectly based strictly on image changes, and delineating fine joint surface structures is difficult. Using a laser, COL1 can be differentiated from COL2. This method is thus suited for assessing tissue properties.

tissue-engineered cartilage tissues cultured for various periods (up to 12 weeks) were used as samples. By comparing the results of biochemical analyses and biomechanical studies, we confirmed the photoacoustic signal as a good indicator for evaluating extracellular matrix formation in order to determine the characteristics of tissue-engineered cartilage [29–38]. We also developed a method for extracellular matrix characterization using TR-LIFS, which enabled simultaneous measurements with mechanical properties using the photoacoustic method [39–41].

We propose the application of these unique measurements and evaluation methodologies [29–41], which we have developed in vitro to non-invasively assess regenerating cartilage (tissue-engineered cartilage) and to diagnose cartilage degeneration. When used in clinical settings, our laser measurement method requires arthroscopy, but the amount of information obtained is greater than that provided by other devices (Table 1). This method may thus be a useful assessment technique in clinical studies that closely assess cartilage.

MATERIALS AND METHODS

Scattering, reflection, and increase in temperature attributable to absorption and the production of fluorescence and acoustic waves are regarded as the main effects when light or laser beams irradiate living organs to be measured (Fig. 1) [42]. A non-invasive and selective diagnostic device that uses optics via a fiber optic cable has recently attracted attention. This device is based on a technology that takes advantage of interactions between optics and living organs. Use of these interactions enables simultaneous collection of not only morphological information, but also various physiological and biochemical data, so the potential for use as a diagnostic device is greater than that of techniques based on a single type of information, such as ultrasonic waves. Bioinstrumentation and imaging with a laser beam, which have recently attracted attention, show features that facilitate the application of this technology to medical fields. We have focused on the interactions between living organs and optics (particularly photoacoustic waves and fluorescence), measured a variety of parameters related to these interactions when induced by the same laser, and developed a system that allows the simultaneous evaluation of the mechanical characteristics and properties of tissue (Fig. 2) [32,33,38].

Evaluation of Mechanical Characteristics Using a Photoacoustic Method

Tissue viscoelasticity affects the propagation and attenuation of the stress waves induced by pulsed laser irradiation [29]. The relaxation time of the stress wave, calculated as the time in which the amplitude of the stress wave decreases by a factor of $1/e$, gives the intrinsic relaxation parameters (η/G) of the tissue, where η is the viscosity and G is the elasticity. We have proposed a basic principle whereby the mechanical characteristics of the tissue can be measured using photoacoustic parameters. In this measurement technique, the relaxation time of the

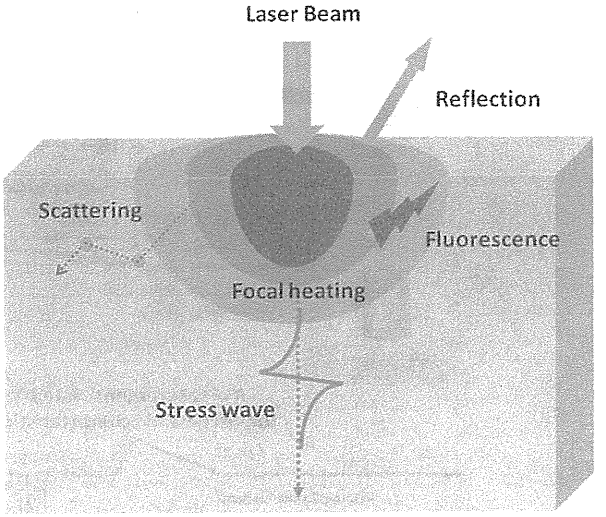

Fig. 1. Mutual interaction between light and a living body. The scattering, reflection, and increase in temperature attributable to absorption and the production of fluorescence and acoustic waves are regarded as the main effects when light or laser beams irradiate living organs to be measured. The figure was cited and modified from Bioengineering: Principles, Methodologies, and Applications ISBN: 978-1-60741-762-0 Authors: M. Sato et al., Editors: A. Garcia et al., pp. 179–190, 2010 Nova Science Publishers, Inc. Chapter 7.

stress that acts on a linear viscoelastic object (consisting of a spring and a dashpot) is related to the viscoelastic parameters of the object, and to the damping time of the stress waves generated by irradiation with a nanosecond pulse laser. Relaxation time is theoretically related to the viscoelastic ratio [42]. The relaxation time (τ) is calculated using the Levenberg–Marquardt algorithm, a nonlinear least-squares method, as follows. When the stress wave intensity is attenuated only by its reflection at the boundaries and its relaxation during its transmission through viscoelastic materials, then the time course of the stress wave intensity is expressed by the following equation [34]:

$$I_\delta = I_0 \times R \times \exp\left(\frac{-t_\delta}{\tau}\right),$$

where I_0 is the intensity of the stress wave at $t = 0$, R is the product of reflectivity (the product of the internal reflectivity at the interface at both ends of the sample), t_δ is the time after laser irradiation, and τ is the damping time of the stress wave and corresponds to the viscoelastic ratio.

As the optimum wavelength of the laser beam was unknown at the beginning of this study, we used an optical parametric oscillator (Spectra-Physics, Tokyo, Japan) with the original probe (Fig. 3) and set the oscillation wavelength within the range of 250–355 nm, with collagen and protein as the optical absorbers.

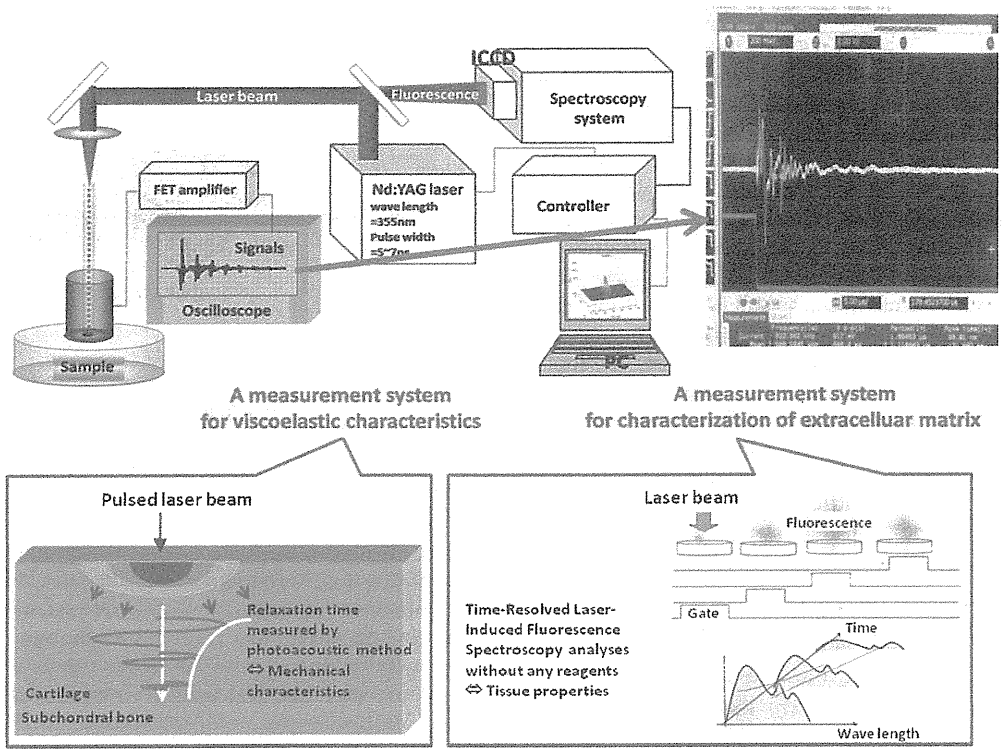

Fig. 2. Simultaneous measurement system: photoacoustic measurement of viscoelastic characteristics and fluorescent measurement with time-resolved autofluorescence spectroscopy. From a practical perspective, a commercially available 3rd (355 nm) harmonic Q-switched Nd:YAG laser (pulse width, 5–6 nanoseconds) was used for the excitation light source in the present study. The light beam was focused with a lens and then coupled to a silica fiber of 400 μm in core diameter. Transmitted light energy was maintained at approximately 50 μJ/pulse. Thermoelastic waves induced by the light pulses were detected by a piezoelectric transducer we designed ourselves, which consisted of a P(VdF/TrFE) film of 55 μm in thickness. Output signals of the transducer were amplified with a low-noise amplifier (bandwidth, 1 kHz–100 MHz; gain, 46 dB) and acquired with a multi-channel digital oscilloscope (bandwidth, 1 GHz). The relaxation time, calculated as the time for the thermoelastic wave amplitude to decrease by a factor of $1/e$, gave the relaxation parameters (η/G) of tissue, where η is viscosity and G is elasticity. Time-resolved fluorescent spectroscopy was obtained by a photonic multi-channel analyzer with intensified CCD. For time-resolved measurement, a trigger signal was controlled by a 4-channel digital signal generator. Fluorescent features of the developed measurement system are as follows: wavelength range, 200–860 nm; wavelength resolution <3 nm; exposure time, 19 milliseconds; gate time, 10 nanoseconds. The parameters of measured fluorescence, obtained using MatLab software, were peak wavelength at fluorescence maximum, fluorescent spectral bandwidth at half-maximal amplitude (FWHM), and integrated intensity of time-resolved spectrum. The figure was cited and modified from Bioengineering: Principles, Methodologies, and Applications ISBN: 978-1-60741-762-0 Authors: M. Sato et al., Editors: A. Garcia et al., pp. 179–190, 2010 Nova Science Publishers, Inc. Chapter 7.

Safety Test

To assess the safety of the photoacoustic measurement method, we used a cell proliferative activity test in cultivated domestic rabbit chondrocytes and examined the effects on chondrocytes of laser beam irradiation to induce photoacoustic signals. As irradiation conditions of the laser were based on the third harmonic frequency of a Q switch Nd:YAG laser with a wavelength of 355 nm, the following five groups were established and examined: (1) a group treated under clinically used radiation conditions (100 μJ/mm^2, 30 shots, $n = 6$); (2) a group treated under conditions in which the pulse energy was 1.5-times greater than that used clinically (150 μJ/mm^2, 30 shots, $n = 6$); (3) a group treated under conditions in which the number of pulse shots was 50 times higher than the

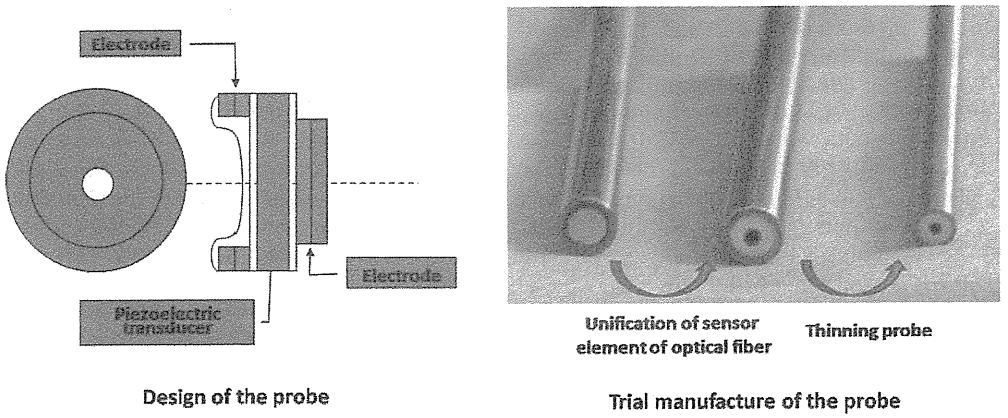

Fig. 3. Development of the probes. We developed a probe in which the optical output was introduced via a quartz glass optical fiber (core diameter 400 nm; Thorlabs Japan), and the P (VdF/TrFE) of a piezoelectric polymer film was used to detect the photoacoustic waves. In this polymer film, the laser irradiation side and the measuring side were originally opposite, so only transparent objects could be evaluated in vitro. However, with repeated trial and error, we developed an integrated optical fiber reflective probe that allowed measurements to be made in vivo, specifically during arthroscopy, by situating the probe at the center and placing the sensors peripherally around it in a circle. The figure was cited and modified from Bioengineering: Principles, Methodologies, and Applications ISBN: 978-1-60741-762-0 Authors: M. Sato et al., Editors: A. Garcia et al., pp. 179–190, 2010 Nova Science Publishers, Inc. Chapter 7.

number used clinically (150 μJ/mm^2, 1,500 shots, $n = 6$); (4) a positive control group to which 70% ethanol was added to completely kill the cells ($n = 4$); and (5) a negative control with no laser irradiation ($n = 4$). Notably, the pulse energy used to treat group (2) represented the maximum output of this device. A WST-8 assay (Dojindo Laboratories, Kamimashiki, Kumamoto, Japan) was used for the cell proliferative activity test. We applied the abovementioned conditions to cultivated cells sown in a 96-well plate and cultured at 37°C under 5% CO_2, with all measurements made after 1 hour.

Comparative Studies of Mechanical Properties for Tissue-Engineered Cartilage Measured by Photoacoustic Method and Intrinsic Viscoelastic Measurements

Tissue-engineered cartilage made from chondrocytes cultured using scaffold. Twelve knee joints were obtained from 4-week-old female Japanese White rabbits, each weighing about 1 kg. Articular cartilage was separated from the joint with a scalpel and digested for 4 hours in Dulbecco's modified Eagle's medium (DMEM) (Nissui Pharmaceutical, Tokyo, Japan) containing 0.0125% (w/v) bacterial collagenase P (Roche, Mannheim, Germany) and 0.05% actinase E (Kaken Pharmaceutical, Tokyo, Japan). The digested tissue was passed through a cell strainer (BD Biosciences, Wobum, MA) with a pore size of 40 μm. The filtrate was centrifuged at 1,500 rpm for 10 minutes to separate the cells. Cells were then seeded at high density (1×10^6 cells per scaffold) into an ACHMS scaffold (atelocollagen honeycomb with a membrane seal; diameter, 11 mm; thickness, 2 mm) [41,43,44], which we

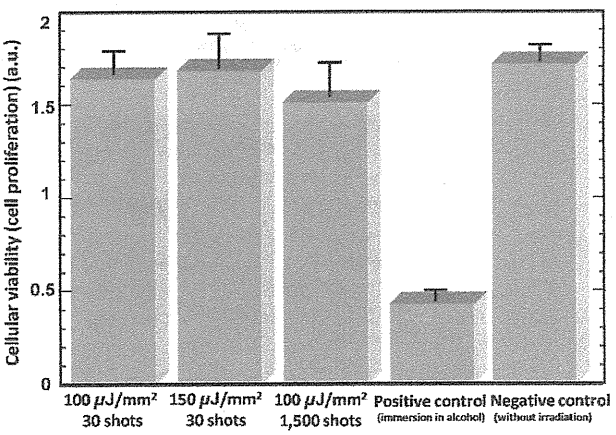

Fig. 4. Effect of laser irradiation (energy per mm^2) on cell viability (cell proliferation). Results of a cell proliferation assay using WST-8. Data were obtained 1 hour after incubation and inoculation. Group A: 100 mJ/mm^2, 30 shots (this condition is standard in our studies). Group B: 150 mJ/mm^2, 30 shots (this condition represents maximum fluence of this laser system). Group C: 100 mJ/mm^2, 1,500 shots. Group D: Positive control (immersion in alcohol). Group E: Negative control without irradiation. Error bars show standard deviation ($n = 4$–6). Results for Group E showed no significant differences from those for the other laser irradiation groups (Groups A–C). The figure was cited and modified from Lasers in Surgery and Medicine 38:249–255 (2006) Authors: M. Ishihara, M. Sato et al.

had developed for three-dimensional and high-density culture in 48-well plates (Sumitomo Bakelite, Tokyo, Japan) by centrifugation at 500 rpm for 5 minutes and then cultured in DMEM-F12 (Iwaki, Tokyo, Japan) supplemented with 10% fetal bovine serum at 37°C in an atmosphere of 5% CO_2 in air and 100% relative humidity. After the indicated periods of incubation, tissue-engineered cartilages using ACHMS scaffold (Fig. 5) were studied biomechanically using the photoacoustic method ($n = 6$) and intrinsic viscoelastic measurements ($n = 6$).

Biomechanical Study

Photoacoustic method. The third harmonic frequency of a Q switch Nd:YAG laser (wavelength, 355 nm; pulse width, 5–6 nanoseconds; Excel Technology, Tokyo, Japan) was used at a constant repetition rate of 10 Hz. The beam was focused using a lens and then coupled to a silica fiber with a core diameter of 400 μm. Transmitted light energy was maintained at approximately 50 μJ/pulse. Stress waves induced by the light pulses were detected at the back surface of the sample by a piezoelectric transducer consisting of P(VdF/TrFE) film, 4 mm in diameter and 55 μm in thickness. Output signals of the photoacoustic transducer were amplified using a low-noise amplifier (bandwidth, 1 kHz–100 MHz; gain, 46 dB) and acquired with a multichannel digital oscilloscope (bandwidth, 1 GHz). Relaxation time T, which was calculated as the time required for stress wave amplitude to

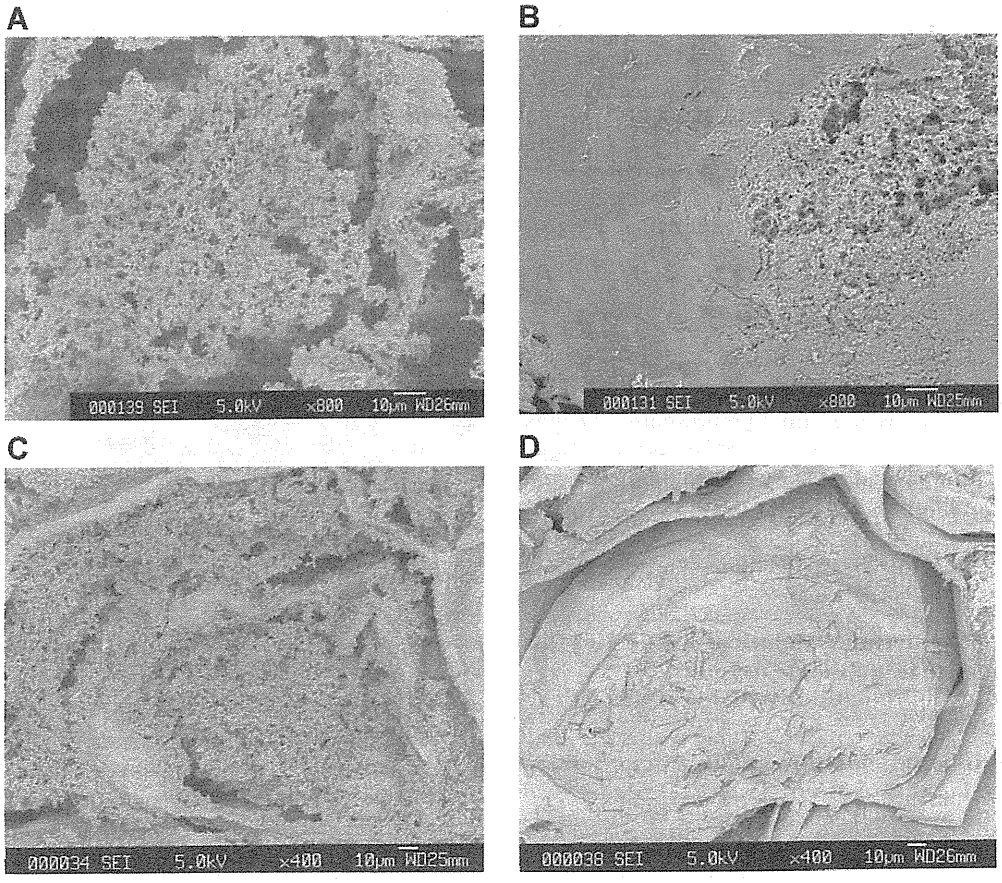

Fig. 5. Tissue-engineered cartilage using ACHMS scaffold. This figure shows a comparison of scanning electron microscopic (SEM) images of tissue-engineered cartilage cultured for 3 and 12 weeks. The lower magnification image of cartilage cultured for 3 weeks (**C**) shows a loose extracellular matrix in the honeycomb-shaped partition. In the higher-magnification image of cartilage cultured for 3 weeks (**A**), a network of collagen fibrils and interspersed proteoglycan is shown. In the images of cartilage cultured for 12 weeks (**B** and **D**), a tight extracellular matrix in the honeycomb partition is shown. Images differ considerably from those of cartilage cultured for 3 weeks, in which collagen and proteoglycan cannot be distinguished. Formation of an extracellular matrix is obvious. The figure was cited from Tissue Engineering Volume 11, Number 7/8, 2005, Mary Ann Liebert, Inc. Authors: M. Ishihara, M. Sato et al.

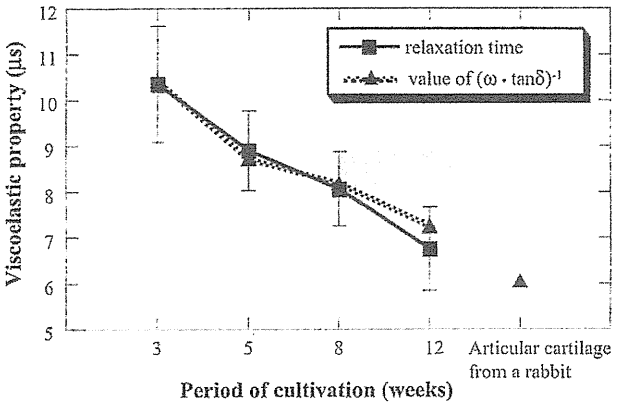

Fig. 6. Comparison of relaxation times measured by the photoacoustic method and values of $(\omega \cdot \tan \delta)^{-1}$ (intrinsic viscoelastic properties) measured with a rheometer as a function of culture time ($\omega = 0.75$ MHz). (■) Relaxation times; (▲) values of $(\omega \cdot \tan \delta)^{-1}$. The correlation coefficient is 0.98. Error bars indicate the standard deviation. To compare viscoelasticities of engineered tissue and native tissues, the value of $(\text{cotan } \delta)^{-1}$ for articular cartilage from a rabbit is plotted ($n = 6$). The figure was cited and modified from Tissue Engineering Volume 11, Number 7/8, 2005, Mary Ann Liebert, Inc. Authors: M. Ishihara, M. Sato et al.

decrease by a factor of $1/e$, was measured. Relaxation time shows a relationship with the viscous-to-elastic modulus rate (tan δ) when ω is defined as the frequency of a stress wave: $T = (\omega \cdot \tan \delta)^{-1}$ [31].

Intrinsic viscoelastic measurements. Intrinsic viscoelastic properties of the same samples as those used for the photoacoustic measurements were examined with a rheometer, a conventional viscoelastic analyzer, and the data were compared to those obtained using the photoacoustic method. Measurements using a rheometer were made at an environmental temperature of 20°C and an initial stress of 80 Pa [31].

The recorded waveform of the photoacoustic signal of the engineered cartilages cultured for 12 weeks is shown in the monitor of a digital oscilloscope in Figure 2. The signal shows a pulse sequence that is due to multiple acoustic reflections at the acoustic boundaries. When attenuation of the stress wave intensity is affected only by reflection at the boundaries and relaxation during transmission through the viscoelastic material, the peak intensity of each wave packet is expressed as an exponential function. Using the Levenberg–Marquardt algorithm, a nonlinear least-squares method, relaxation time can be derived as the time for the stress wave intensity to decrease by a factor of $1/e$.

Evaluation of degenerated cartilage. To produce experimentally degenerated cartilage, we created cartilage with different degrees of degradation by extracting 22 osteochondral plugs (diameter, 12 mm) from four swine patellar cartilage and processing them with trypsin (trypsin-1 × EDTA; Invitrogen, Carlsbad, CA) to cause an outflow of proteoglycan, reflecting changes in the mechanical characteristics of the tissue in vivo. Trypsin was applied for up to 24 hours at a concentration of 1 mg/ml. We assessed degenerated cartilage using the photoacoustic measurement method. After measurements had been made, samples were fixed in 10% formalin solution for histological study. Samples (0 hours: $n = 6$, 6 hours: $n = 6$, 12 hours: $n = 6$, 24 hours: $n = 4$) were sectioned to 4-μm thick slices for microscopic observation and stained with toluidine blue.

Evaluation of Osteochondral Defects in Rabbit Articular Cartilage Using Photoacoustic Measurement Method

We demonstrated the capability of photoacoustic measurement for viscoelastic characterization. Since tissue viscoelasticity affects the propagation and attenuation of photoacoustic waves generated in the tissue, the relaxation times of the photoacoustic waves give the viscoelastic ratio of the tissue. The relaxation times of photoacoustic waves of articular cartilage tissues engineered under various culture conditions were closely correlated with intrinsic viscoelastic ratio measured by using a conventional viscoelastic analyzer ($R > 0.98$, Fig. 6). In order to apply the photoacoustic measurement method to evaluation of the regeneration of articular cartilage as a method to validate the surgery, the method should enable not only evaluation of engineered tissue during cultivation in vitro but also evaluation after transplantation of engineered tissue in vivo. We performed regenerative medicine using the rabbit osteochondral defect model and tissue engineered cartilage using ACHMS scaffold ($n = 8$, Fig. 5).

Evaluation of Cartilage Using Time-Resolved Autofluorescence Spectroscopy

For time-resolved autofluorescence spectroscopy, we used the third harmonic frequency of the Q switch Nd:YAG laser for the excitation light introduced via an optic fiber, in a manner similar to that used in the photoacoustic measurement method. We used a charge-coupled device (CCD) sensor with an image intensifier as the photodetector, while controlling the spectroscopic system that could be measured by a nanosecond order with a 4-channel digital pulse generator. Fluorescence peak intensity, half bandwidth, peak wavelength, fluorescence volume, and fluorescence life were calculated as the measurement parameters. The articular cartilage of Japanese white domestic rabbits ($n = 4$), the outer layer of the annulus fibrosus ($n = 4$), and commercially available type I and type II collagen (powder; Ieda Chemical, Tokyo, Japan, $n = 4$, respectively) were used as the target samples.

RESULTS

Determination of Optimal Wavelength

Photoacoustic signals could thus be measured at any wavelength within this range [29,31]. The shorter wavelengths within this range can magnify absorption by

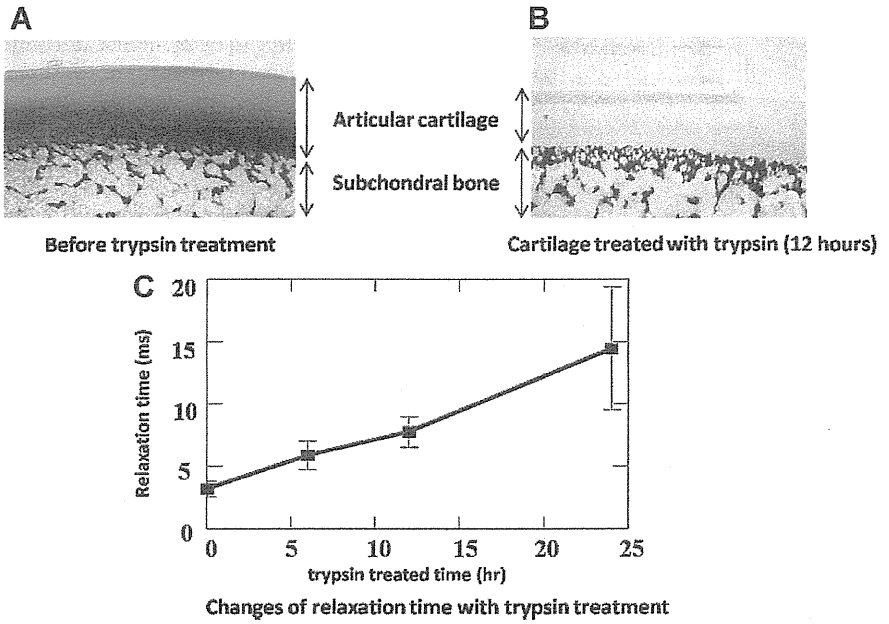

Fig. 7. Photoacoustic evaluation of characteristic viscoelastic changes with cartilage degeneration. Trypsin treatment of the tissue caused marked loss of proteoglycans in the cartilage, as shown in A and B. (a) Toluidine blue staining of a normal porcine cartilage specimen. (b) Toluidine blue staining of a cartilage specimen treated with trypsin for 12 hours. The specimen shows an extensive loss of proteoglycans in the tissue. Changes in the extracellular matrix simultaneously caused change in viscoelasticity of the cartilaginous tissue. The degree of change in viscoelasticity corresponded to the degree of change in the extracellular matrix. C: Relaxation times measured by the photoacoustic measurement method as a function of trypsin treatment time (hours). Error bars show standard deviation (0 hours: $n = 6$, 6 hours: $n = 6$, 12 hours: $n = 6$, 24 hours: $n = 4$). The figure was cited and modified from Lasers in Surgery and Medicine 38:249–255 (2006) Authors: M. Ishihara, M. Sato et al.

living organs, so peak values of the initiated photoacoustic waves can be increased and the initiation depth of the photoacoustic wave set at a shallower level. However, in practical terms, a small, portable, and inexpensive excitation light source is desirable, so we devised a system in which the third harmonic frequency of a Q switch Nd:YAG laser (wavelength, 355 nm; pulse width, 5–6 nanoseconds; Excel Technology) was used [39,40]. We developed a probe in which the optical output was introduced via a quartz glass optical fiber (core diameter, 400 nm; Thorlabs Japan, Tokyo, Japan), and the poly(polyvinylidene fluoride) copolymer (P(VdF/TrFE)) of a piezoelectric polymer film (Nishiki Trading Company, Tokyo, Japan) was used to detect the photoacoustic waves [40]. In this polymer film, the laser irradiation side and measuring side were originally opposite, so only transparent objects were able to be evaluated in vitro. However, with repeated trial and error, we developed an integrated optical fiber reflective probe that allowed measurements to be taken in vivo, specifically during arthroscopy, by situating the probe at the center and placing the sensors peripherally around the probe in a circle (Fig. 3).

Effect of Laser Irradiations

We confirmed a lack of significant differences between any laser-irradiated group and the non-irradiated group, and found that laser irradiation in this study had no effect on cell proliferative activity (Fig. 4) [40].

Mechanical Properties of Tissue-Engineered Cartilage Measured by Photoacoustic Method and Intrinsic Viscoelastic Measurements

In Figure 6, relaxation times are compared to intrinsic viscoelastic parameters (tan δ) measured with a rheometer. The intrinsic relaxation parameter of native cartilage measured with the rheometer is also plotted in Figure 6. Tissue-engineered cartilage cultured for a longer period showed smaller relaxation times. The relaxation times obtained by photoacoustic measurement agreed well with the measured intrinsic relaxation parameters, with a correlation coefficient of 0.98. Compared to native cartilage,

cartilage cultured for the longest period (12 weeks) showed an 85% smaller viscoelastic parameter [31].

Photoacoustic Evaluation of Characteristics of Degenerated Cartilage

Figure 7 shows the positive correlation between damping time and trypsinization time [40]. Specifically, damping time increased with increasing trypsinization time. In other words, viscosity increased and elasticity decreased. Histologically, the stainability of tissue with toluidine blue also decreased with trypsinization and the loss of proteoglycans, suggesting that the course of tissue changes involved in cartilage degeneration can be monitored using the photoacoustic measurement method.

Monitoring the Post-Operative Regenerative Process of Articular Cartilage Using Photoacoustic Measurement Method

We confirmed that the usefulness of the photoacoustic method for repeated measurement of viscoelastic properties of regenerative articular cartilage after allografted tissue-engineered cartilage. The photoacoustic measurements enabled the determinations of viscoelasticities of regenerative cartilage during the total time course after surgery (Fig. 8).

Compositional Information of Cartilage Using Time-Resolved Autofluorescence Spectroscopy

The articular cartilage exhibited a spectrum close to that of type II collagen, and peak wavelengths and half bandwidths were also similar [33,38]. Conversely, the outer layer of the annulus fibrosus exhibited a spectrum close to that of type I collagen, and peak wavelengths and half bandwidths were also similar (Fig. 10) [42,43]. This indicates that the collagen composition of tissue can be measured, as collagen is an autofluorescent substance used in vivo in a non-contact manner. This is significant, as the content ratio of type I to type II collagen is particularly important in diagnosing the degree of cartilage degradation.

DISCUSSION

Based on the above results, we applied the photoacoustic measurement method to evaluate the articular cartilage under the arthroscopy. We received the approval of the Institutional Review Board of Tokai University Hospital concerning the photoacoustic measurement method, and applied the method to some kinds of arthroscopic surgeries. The surgeon can easily have a true figure of photoacoustic waveform using the real-time monitoring. The measuring photoacoustic waveform in the monitor can be changed to make larger or smaller by switching (Fig. 9). The measurable thickness was limited from approximately 1.5 to 6 mm in the present experimental condition. In this range of the cartilage thickness, the effect of the thickness on the accuracy of the measurement was ignorable.

Many elderly people who suffer from lifestyle-related diseases are also affected by osteoarthritis and are often unable to perform exercises that would normally be within their physical capacity, due to joint pain and limited range of motion. This is particularly serious in patients with diabetes, hyperlipidemia, or obesity, and the disease may be exacerbated because osteoarthritis reduces the ability to exercise, even when exercise therapy is available. In osteoarthritis, evaluating the prognosis of conservative therapy or the treatment effects after surgery often depend on the symptoms of the

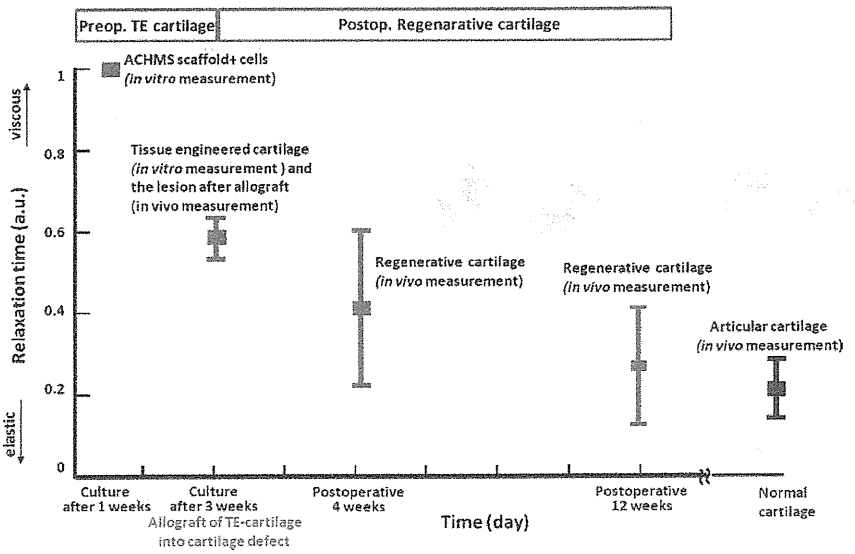

Fig. 8. The results of photoacoustic measurement of pre- and post-operative cartilage. A total time course of pseudo-regenerative medicine using rabbit model was able to be monitored by photoacoustic method.

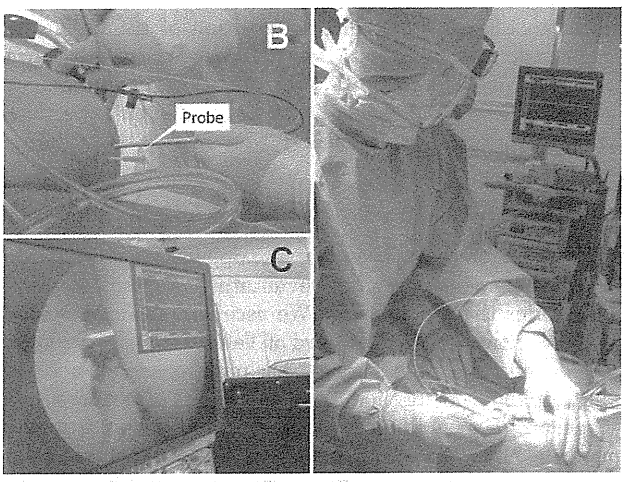

Fig. 9. Clinical application of photoacoustic measurement. **A**: The measuring photoacoustic waveform can be checked by the monitor of arthroscopy. **B**: The integrated optical fiber of reflective probe was 4mm in diameter (Fig. 3). **C**: The measuring photoacoustic waveform in the monitor can be changed to make larger or smaller by switching.

patient, so the pathological condition is not accurately understood. Surgical treatments such as artificial joint replacement are currently performed on patients in the terminal phase, whereas patients in the initial to middle phases are treated conservatively, often without any clear aims.

The present studies have demonstrated that the mechanical characteristics and properties of articular cartilage can be evaluated simultaneously during arthroscopy using a non-invasive intense pulsed laser (Table 1). We are now developing a device for this application by trial and error. If such a device is developed, accurate measurement of the mechanical characteristics involved with the original function of the articular cartilage and the associated tissue properties will be possible during arthroscopy, and anyone could perform such quantitative functional evaluations. This will enable an accurate understanding of the pathological features of osteoarthritis and careful planning and implementation of treatments. This technology could also allow quantitative measurement and evaluation of mechanical characteristics and tissue properties simultaneously, to assess treatment effects such as those of a variety of drugs, in

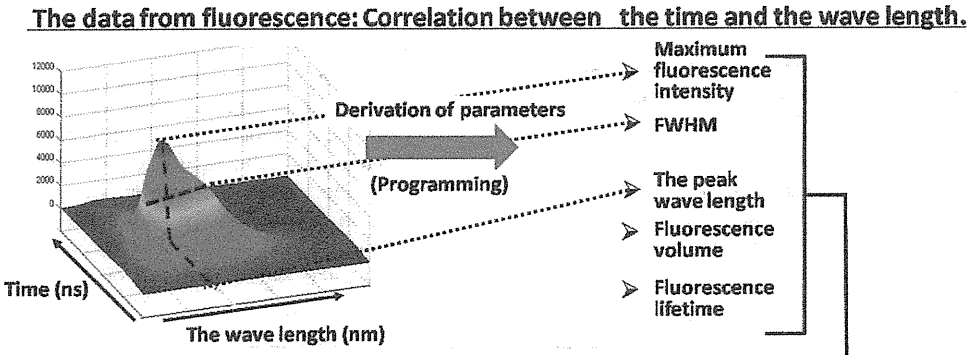

An evaluation of multiple characteristics from several parameters.

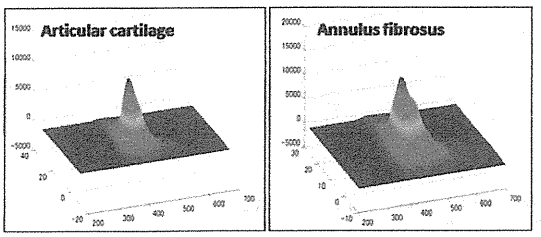

	The peak wave length (nm)	FWHM (nm)
Articular cartilage	398	64.2
Annulus fibrosus	443	120
Type 2 collagen	401	65.7
Type 1 collagen	438	120

Fig. 10. Analyses with time-resolved autofluorescence spectroscopy. Fluorescence peak intensity, full width at half maximum (FWHM), peak wavelength, fluorescence volume, and fluorescence life were calculated as the measurement parameters. The articular cartilage of Japanese white domestic rabbits, the outer layer of the annulus fibrosus, and commercially available type I and type II collagen were used as target samples. Articular cartilage exhibited a spectrum close to that of type II collagen, and peak wavelengths and half bandwidths were also similar. Conversely, the outer layer of the annulus fibrosus exhibited a spectrum close to that of type I collagen, and peak wavelengths and half bandwidths were also similar. This indicates that the collagen composition of tissue can be measured, as collagen is an autofluorescent substance used in vivo in a non-contact manner. The figure was cited and modified from Bioengineering: Principles, Methodologies, and Applications ISBN: 978-1-60741-762-0 Authors: M. Sato et al., Editors: A. Garcia et al., pp. 179–190, 2010 Nova Science Publishers, Inc. Chapter 7.

addition to the conventional evaluation of clinical symptoms such as pain or inflammation around the joints. We believe that this methodology will be useful in the objective evaluation of articular cartilage in investigations such as clinical trials of new drugs. This diagnostic system is a methodology used during arthroscopy, and so cannot be a completely non-invasive evaluation [41]. However, if quantitative data are collected during arthroscopy treatments, the effects of a variety of conservative therapies will be able to be predicted, based on the severity of cartilage degeneration. Planning and performance of treatments on an individual basis will thus be possible. Accordingly, we are certain that the development of this technology and practical diagnostic devices will improve activities of daily living and quality of life for patients, and thus contribute to a healthy life expectancy.

CONCLUSION

1. A photoacoustic measurement method using a non-invasive nanosecond-pulsed laser allows evaluation of the mechanical characteristics of cartilage, and time-resolved autofluorescence spectroscopy allows the evaluation of tissue properties for analysis.
2. This measurement system, based on interactions between optics and living organs, is an evaluation methodology suitable for making diagnoses during arthroscopy.

ACKNOWLEDGMENTS

This work was supported by the Takeda Science Foundation, the General Insurance Association of Japan, Mitsui Sumitomo Insurance Welfare Foundation, a High-Tech Research Centre Project for Private Universities, a grant-in-aid for Scientific Research from the Ministry of Education, Culture, Sports, Science, and Technology of Japan, the New Energy and Industrial Technology Development Organization, and the Japan Foundation for Aging and Health.

REFERENCES

1. Yoshimura N, Oka T, Muraki S, Mabuchi A, Enyo Y, Yoshida M, Kawaguchi H, Nakamura K. Epidemiology of osteoarthritis in Japan. J Jpn Orthop Assoc 2007;81:17–21.
2. Modest VE, Murphy MC, Mann RW. Optical verification of a technique for in situ ultrasonic measurement of articular cartilage thickness. J Biomech 1989;22:171–176.
3. Rushfeldt PD, Mann RW, Harris WH. Improved techniques for measuring in vitro the geometry and pressure distribution in the human acetabulum-I. Ultrasonic measurement of acetabular surfaces, sphericity and cartilage thickness. J Biomech 1981;14:253–260.
4. Kim HK, Babyn PS, Harasiewicz KA, Gahunia HK, Pritzker KP, Foster FS. Imaging of immature articular cartilage using ultrasound backscatter microscopy at 50 MHz. J Orthop Res 1995;13:963–970.
5. Adler RS, Dedrick DK, Laing TJ, Chiang EH, Meyer CR, Bland PH, Rubin JM. Quantitative assessment of cartilage surface roughness in osteoarthritis using high frequency ultrasound. Ultrasound Med Biol 1992;18:51–58.
6. Laasanen MS, Töyräs J, Hirvonen J, Saarakkala S, Korhonen RK, Nieminen MT, Kiviranta I, Jurvelin JS. Novel mechano-acoustic technique and instrument for diagnosis of cartilage degeneration. Physiol Meas 2002;23:491–503.
7. Nieminen HJ, Töyräs J, Rieppo J, Nieminen MT, Hirvonen J, Korhonen R, Jurvelin JS. Real-time ultrasound analysis of articular cartilage degradation in vitro. Ultrasound Med Biol 2002;28:519–525.
8. Toyras J. Quantitative evaluation of spontaneously and surgically repaired rabbit articular cartilage using intra-articular ultrasound method in situ. Ultrasound Med Biol 2010;36:833–839.
9. Bader DL, Kempson GE. The short-term compressive properties of adult human articular cartilage. Biomed Mater Eng 1994;4:245–256.
10. Korhonen RK, Laasanen MS, Toyras J, Lappalainen R, Helminen HJ, Jurvelin JS. Fibril reinforced poroelastic model predicts specifically mechanical behavior of normal, proteoglycan depleted and collagen degraded articular cartilage. J Biomech 2003;36:1373–1379.
11. Froimson MI, Ratcliffe A, Gardner TR, Mow VC. Differences in patellofemoral joint cartilage material properties and their significance to the etiology of cartilage surface fibrillation. Osteoarthritis Cartilage 1997;5:377–386.
12. Maroudas A, Evans H, Almeida L. Cartilage of the hip joint. Topographical variation of glycosaminoglycan content in normal and fibrillated tissue. Ann Rheum Dis 1973;32:1–9.
13. Hattori K, Mori K, Habata T, Takakura Y, Ikeuchi K. Measurement of the mechanical condition of articular cartilage with an ultrasonic probe: Quantitative evaluation using wavelet transformation. Clin Biomech (Bristol, Avon) 2003; 18:553–557.
14. Hattori K, Ikeuchi K, Morita Y, Takakura Y. Quantitative ultrasonic assessment for detecting microscopic cartilage damage in osteoarthritis. Arthritis Res Ther 2005;7:R38–R46.
15. Appleyard RC, Swain MV, Khanna S, Murrell GA. The accuracy and reliability of a novel handheld dynamic indentation probe for analysing articular cartilage. Phys Med Biol 2001;46:541–550.
16. Bae WC, Temple MM, Amiel D, Coutts RD, Niederauer GG, Sah RL. Indentation testing of human cartilage: Sensitivity to articular surface degeneration. Arthritis Rheum 2003; 48:3382–3394.
17. Lyyra T, Jurvelin J, Pitkänen P, Väätäinen U, Kiviranta I. Indentation instrument for the measurement of cartilage stiffness under arthroscopic control. Med Eng Phys 2003;17: 395–399.
18. Viren T, Saarakkala S, Kaleva E, Nieminen HJ, Jurvelin JS, Toyras J. Minimally invasive ultrasound method for intra-articular diagnostics of cartilage degeneration. Ultrasound Med Biol 2009;35:1546–1554.
19. Huang YP, Zheng YP. A potential arthroscopic tool for quantitative assessment of articular cartilage. Open Biomed Eng J 2009;26:13–20.
20. Viren T, Saarakkala S, Jurvelin JS, Pulkkinen HJ, Tiitu V, Valonen P, Kiviranata I, Lammi MJ, Xia Y, Moody JB, Burton-Wurster N, Lust G. Quantitative in situ correlation between microscopic MRI and polarized light microscopy studies of articular cartilage. Osteoarthritis Cartilage 2001; 9:393–406.
21. Li X, Martin S, Pitris C, Ghanta R, Stamper DL, Harman M, Fujimoto JG, Brezinski ME. High-resolution optical coherence tomographic imaging of osteoarthritic cartilage during open knee surgery. Arthritis Res Ther 2005;7:R318-23.
22. Chu CR, Izzo NJ, Irrgang JJ, Ferretti M, Studer RK. Clinical diagnosis of potentially treatable early articular cartilage degeneration using optical coherence tomography. J Biomed Opt 2007;12:051703.
23. Burstein D, Gray M. New MRI techniques for imaging cartilage. J Bone Joint Surg Am 2003;85-A(Suppl 2): 70–77.
24. Nieminen MT, Toyras J, Rieppo J, Hakumäki JM, Silvennoinen J, Helminen HJ, Jurvelin JS. Quantitative MR microscopy of enzymatically degraded articular cartilage. Magn Reson Med 2000;43:676–681.